Fiber optical interferometric sensor based on mechanical oscillation

Peter Lehmann, Markus Schulz, Jan Niehues
Dept. of Electrical Engineering, Chair in Measurement Technology, University of Kassel, Germany

ABSTRACT

For geometry measurement of high precision machined mechanical or optical workpieces a resolution in the nanometer range is generally required. This can be reached by interferometric principles. In addition, measurement at steep flanks can be achieved by optical systems with high numerical apertures. Unfortunately, a high NA is always accompanied by a small depth of focus leading to a very limited measuring range. A possible solution in this context is a so-called depth scan.

We realized a pointwise measuring interferometric sensor and use a piezo driven bending beam for the depth scan. A micro-optical fiber probe with an integrated reference surface is mounted at the top of this beam. By use of a piezoelectric actuator driven close to the resonant frequency of several hundred Hertz the beam deflects with a few micrometers of amplitude. By this oscillation the optical path length of the measuring rays of the interferometer is modulated, while the reference path remains unchanged. This leads to an interference signal which shows characteristic changes in phase as the average distance between optical probe and measuring object changes.

Keywords: Fiber optic sensor, optical profilometry, interferometric principle, oscillating bending beam

1. INTRODUCTION

Although optical instruments show several advantages over tactile geometry measurement in today's industrial applications tactile systems are still dominating. Besides their robustness important features of tactile sensors are their flexibility and relatively low costs.

However, replacing tactile by optical sensors without further changes of the measuring instrumentation would provide a great benefit for industrial users: They could measure optically wherever possible, but if for several reasons tactile measurement is required this can be done with minimum effort.

Current commercially available optical sensors meet some but not all of the requirements of industrial use[1-3]. Besides technical limitations, these systems are generally much more expensive compared to tactile sensors of comparable accuracy. Furthermore, problems occur, for example if steeper flanks of specularly reflecting objects are to be measured optically. Often systematic measuring errors or a complete failure of an optical sensor will be the consequence.

Therefore, it was our motivation to search for a sensor principle, which allows to overcome some of the difficulties and restrictions of existing systems.

For the addressed applications of high precision measurement a height resolution of less than 10 nanometers is necessary. This can be reached by interferometric principles but hardly by confocal or triangulation sensors.

In addition, the capability of measurement at steep flanks depends on the surface roughness of a measuring object under investigation. Whereas for a rough surface a local surface tilt up to 80° may be tolerated by the sensor, for an optically smooth surface the maximum tilt angle strongly depends on the numerical aperture of the sensor optics. A maximum tolerance against surface tilt can be achieved by optical systems with an as big as possible numerical aperture (NA) as it is shown in Fig. 1. Nevertheless, the theoretical limit of surface tilt is given by the angle Θ_{max} corresponding to the numerical aperture:

$$NA = n \sin \Theta_{max} . \tag{1}$$

Furthermore, if surface roughness is to be measured a lateral resolution Δx of less than one micrometer is generally necessary. Since

$$\Delta x \approx \frac{\lambda}{2\,NA}, \tag{2}$$

this requires an as big as possible NA again.

Optical Measurement Systems for Industrial Inspection VI, edited by Peter H. Lehmann, Proc. of SPIE
Vol. 7389, 738915 · © 2009 SPIE · CCC code: 0277-786X/09/$18 · doi: 10.1117/12.827510

On the other hand, a great NA is always accompanied by a small depth of focus d_z or a short Rayleigh length leading to a very limited measuring range:

$$d_z \approx 2\frac{\lambda}{NA^2}. \tag{3}$$

A possible approach to extend the measuring range in this context is to stretch the focus depth by using the longitudinal chromatic aberration [2, 4-7].

A broad variety of industrial confocal chromatic sensors based on this idea are commercially available today. Although some effort was spent to realize micro-optical probes based on this principle by using the chromatic aberration of diffractive elements[4,5] up to now no optical sensor following this approach is ready for industrial use. The reason for this may be given by measurement uncertainties related to the optical properties of the diffractive elements.

A further sensor principle called chromatic confocal spectral interferometry was established at the Institut für Technische Optik, University of Stuttgart, a few years ago[7-9]. They placed a diffractive element in the entrance pupil of a microscope objective in order to achieve a well defined axial chromatic spreading even for greater numerical apertures. An advantage of this approach in comparison with conventional chromatic confocal sensors is that the NA is independent of the wavelength of light. However, the results published so far are based on a high NA microscope objective and a micro-optical realization of the principle might be difficult.

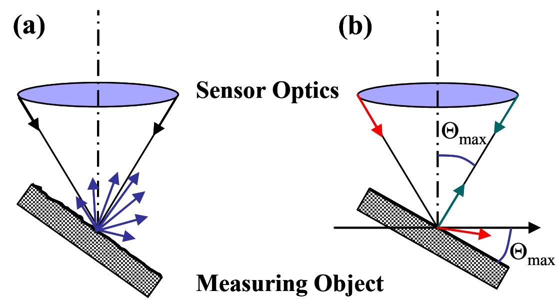

Fig. 1: Optical measurement on a tilted optically rough surface (a) and a smooth surface (b).

2. MEASURING PRINCIPLE AND EXPERIMENTAL SETUP

The interferometer we used for this study is based on a common-path setup in order to keep the system robust. Since the normal of the reference surface corresponds to the optical axis of the micro-optical probe it can be regarded as a Fizeau-configuration. However, it shall be emphasized that the interferometer is a pointwise measuring sensor, i.e. distance changes of on axis object points are measured. The length of the reference arm of the interferometer is always constant, while the optical path length of the measuring arm changes periodically.

2.1 Focus Scanning Approach

This results in the so-called depth scan as an alternative to wavelength coding and spectrometric techniques. The depth scan can be easily performed by using a micro-optical probe with a small depth of focus which is moved up and down with an amplitude corresponding to the required measuring range. The general principle is closely related to a movement of a reference mirror along the optical axis as it is usually employed in time-domain optical coherence tomography (OCT)[9]. However, in contrast to the measuring principle introduced here, time-domain OCT is a coherence scanning method.

It was our approach to realize the depth scan by a piezo driven bending beam. An optical fiber probe with an integrated reference surface is mounted at the top of this beam.

By use of a piezoelectric actuator driven close to the system's resonant frequency of several hundred Hertz the beam deflects with a few micrometers of amplitude. By this oscillation the optical path length of the measuring rays of the interferometer is modulated, while the reference path remains unchanged.

This leads to an interference signal $I(h,t)$ where $t = z/v$ is the time corresponding to the height position z and the speed v of the oscillating beam. z represents the deflection of the bending beam and h is the height position of the reflecting object point. If the average of the distance $h - z$ between optical probe and measuring object is varied the measured interference intensity

$$I(h,t) = I_1 + I_2 + 2\sqrt{I_1\, I_2}\, \cos\left(\varphi_0 + \frac{4\pi}{\lambda}\left[h(x,y) - v\,t \right] \right) \tag{4}$$

shows characteristic changes in the phase, which are to be obtained by an appropriate signal processing algorithm. The intensities I_1 and I_2 are related to the measuring and the reference light, respectively, and λ is the wavelength of light.
If the piezoelectric bending beam is driven by a triangular voltage function the speed v can be assumed to be constant within the measuring range.
As an advantage of this method a common fiber coupled laser diode can be used as a light source and the intensity signal can measured by a simple photo diode.

2.2 Experimental Setup

In Fig. 2 (right hand side) the experimental setup is illustrated schematically; Fig. 2 (left hand side) shows a photograph of the optical probe and the bending beam, which is mounted on an xyz-stage. The fiber probe we used in this first attempt was originally developed for a fiber sensor based on low-coherence interferometry. Since the measuring range of this sensor is limited to the depth of focus the NA of this probe was quite low (approximately 0.11)[10, 11].

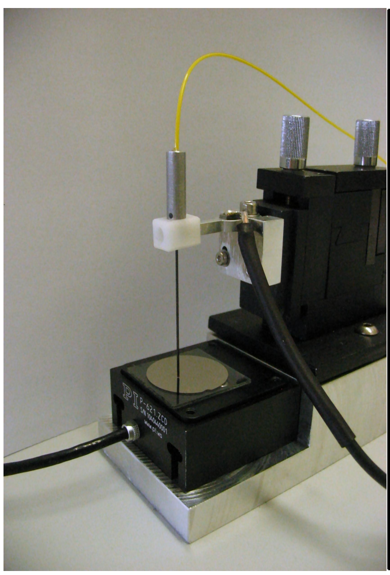

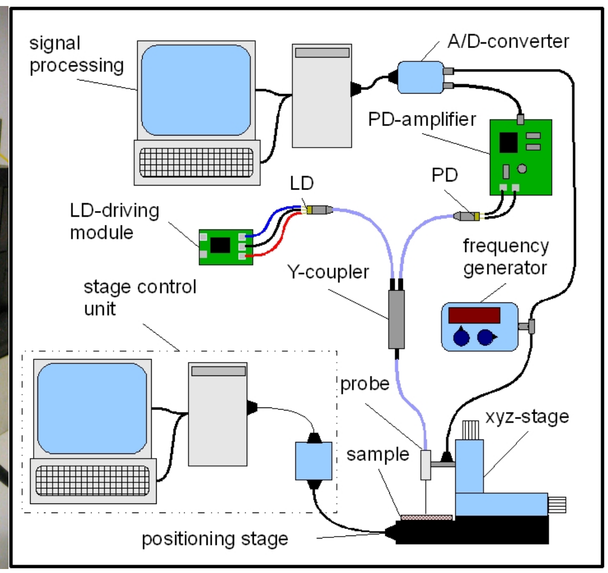

Fig. 2: Photograph of the horizontal bending beam and the vertical optical probe (left), schematic of the measurement setup (right).

The probe design is based on a gradient-index fiber which is spliced to a single-mode fiber. A ferule made of carbon-fiber reinforced plastic (CFP) is used to protect the probe and allows a simple handling. The total probe length and diameter are approximately 50 mm and 0.8 mm, respectively.
The fiber probe is connected via a single mode fiber to the laser diode which emits light at 785 nm wavelength. The reference waves are reflected back from the exit surface of the probe. The measuring rays transmit the exit surface and are focused onto the surface of the object under investigation. A part of this light is reflected from the object, coupled again into the same fiber and propagates back through the fiber. This light as well as the reference light is split by a fiber coupler and the relevant part is directed to a photo diode where it is detected.
A detailed scheme of the probe system is shown in Fig. 3. An electrical voltage at the piezo actuator gives rise to a deflection of the bending beam and the distance between bending beam and the object's surface decreases. As a consequence, a certain number of intensity maxima and minima are measured by the photo diode. For a deflection of Δz the corresponding number of cycles of the interference signal is predicted by Eq. (4).

The measured signals are first amplified and filtered before they are sampled and digitized for numerical evaluation.

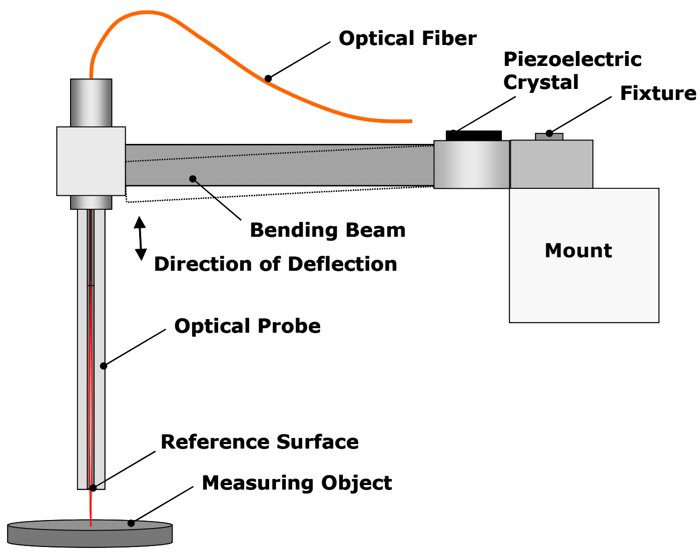

Fig. 3: Scheme of the sensor setup showing the interferometric fiber coupled probe and the piezo-electrically driven bending beam.

2.3 Signal Conditioning and Evaluation

In order to prepare the signals for analog-to-digital conversion, they were amplified in two steps. First, a trans-impedance amplifier is used to convert the photodiode current into a voltage level. Due to the characteristics of this amplifier the diode shows a linear behaviour between light intensity and electric current. According to Eq. (4) the interference term is superimposed by an offset term, which is independent of the optical path difference. Therefore, a selective amplifier with an integrated high pass filter was used in order to get rid of the offset term.

As mentioned above, the bending beam moves down by providing a voltage to the contacts of the piezoelectric crystal. A nearly linear dependence between driving voltage and beam deflection can be achieved by a triangular input signal. The system answers with an approximately harmonic interference signal at the rising and falling flank as it is shown in Fig.4 a). The distance between two neighbouring interference maxima of this signal should be $\lambda/2$ according to Eq. (4).

Next to the peak and the valleys of the triangular function, the interference signal shows a phase jump and a variation of the frequency. This part cannot be used for signal processing. However, the number of interference fringes between a peak and a valley corresponds to the maximum deflection of the bending beam. By increasing the voltage at the piezoelectric crystal a greater deflection could be realized.

For further signal processing, we cut out the harmonic section of the signal and multiply by a window function in order to avoid leakage. Examples of windowed signals in the time domain are shown in Fig. 4 b). These signal sections are then transformed into the frequency domain. In the frequency spectrum a maximum peak height results at the frequency of the interference signal. Consequently, the phase of the signal is obtained at the frequency value, where the maximum power spectral density occurs.

The triangular driving voltage and the interference signal were recorded simultaneously. Therefore, the driving signal can be used as a reference signal. However, there is a need for a precise synchronization of the different measurement intervals. In order to achieve a high accuracy of synchronization the flanks of the driving signal were fitted by straight lines. The points of intersection of these lines were used to trigger the interference signals, i.e. the phase values are related to these reference points. Hence, these points represent the reference for the determination of distance changes.

For this study the piezoelectric crystal was driven by a triangular signal of approximately 1250 Hz and the signals obtained from the photodiode were sampled with a frequency of 200 kHz and digitized with a resolution of 16 bit.

The two signals depicted Fig. 4 b) are phase shifted by approximately 180°. According to Eq. (4) this results in a distance change between measuring object and sensor of 200 nm. However, the distance change produced by a calibrated nano-positioning stage was only 100 nm. An explanation for this discrepancy is given in section 4.

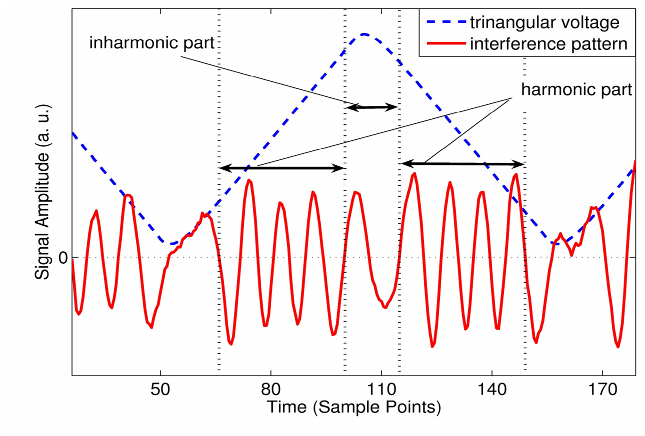

a)

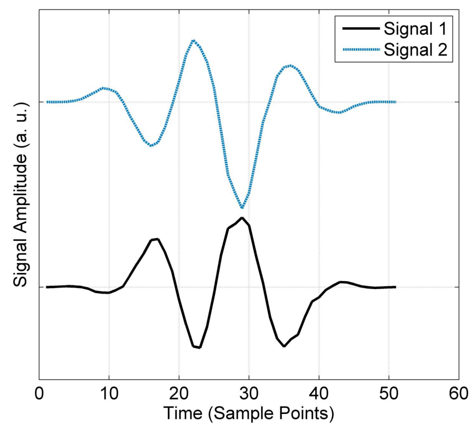

b)

Fig. 4: a) Triangular driving signal and the corresponding interference signal obtained by the oscillating sensor;
b) Signal sections after multiplying by a window function revealing a 180° phase shift due to a distance change of 100 nm.

3. MEASURING RESULTS

3.1 Repeatability

First, repeatability measurements have been carried out in order to characterize the behavior of the oscillating sensor. A number of signals were recorded while the optical probe was oscillating in a constant distance from the measuring object. The measuring object used for these measurements was a chromium layer on a glass substrate.
Fig. 5 (top) shows the measured distance variation of 80 single measurements. In addition, the distance distribution of these measuring results and the fitted Gaussian curve are plotted (Fig. 5, bottom). The standard deviation obtained from these results is 3 nm.

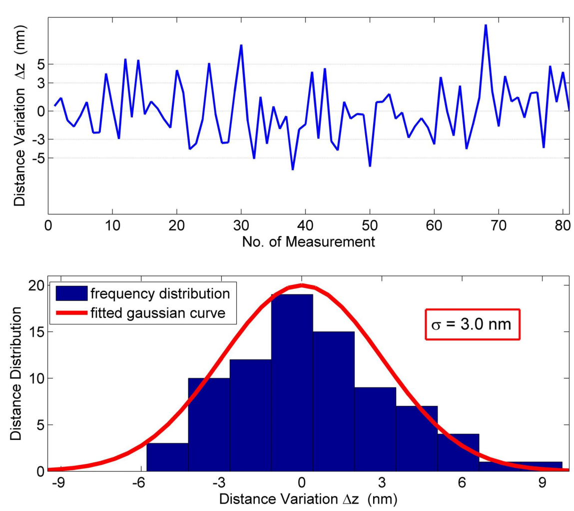

Fig. 5: Results of repeatability measurement showing the uncertainty due to distance changes.

In this context it should be noted that due to its length the optical probe is rather sensitive against vibration disturbances. These either result from a transversal oscillation of the probe generated by the oscillating beam or from environmental vibrations. Consequently, it is to be expected that the standard deviation can be further reduced by optimizing the probe geometry and vibration isolation of the measuring setup.

3.2 Distance Changes

Second, the distance between the sensor and the measuring object was changed in small steps by use of a piezoelectric *z* translation stage with an integrated capacitive sensor. The capacitive sensor was calibrated by means of a length measuring laser interferometer. The measuring uncertainty should be less than 1 nanometer.

Since the measuring object is a perfectly aligned specularly reflecting surface, this arrangement provides ideal conditions in order to check the sensitivity of the sensor. There is no tilt, no curvature, and no edge on the measuring object, which could lead to an increased measuring uncertainty.

The measuring object was moved in the vertical direction towards the optical probe in well-defined steps of 100 nm. The results are shown in Fig. 6. Obviously the sensor works correctly, except for a small jump of approximately 10 nm between measurement no. 150 and 200. Since this offset remains constant over the rest of the measurement series, it is expected that this distance step is caused by a lack of stability of the mechanical fixture.

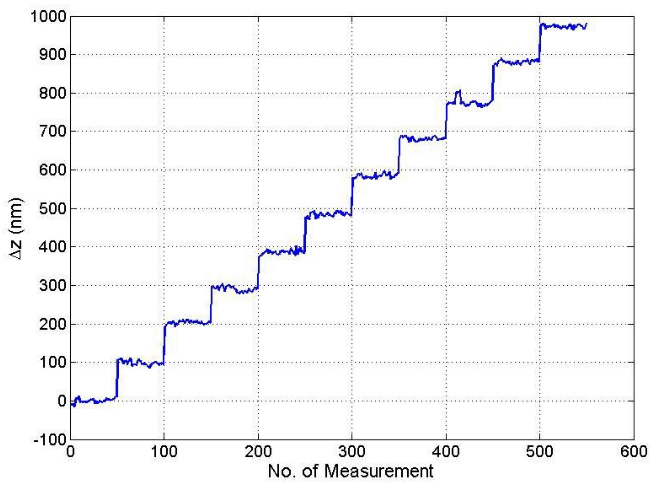

Fig. 6: Measuring results related to 100 nm distance changes between sensor and measuring object.

4. DISCUSSION

In Fig. 4 b) a phase shift of approximately 180° was established for a distance change between probe and sample of only 100 nm. This is twice the phase difference, which was expected according to Eq. (4). However, the optical probe can also be regarded as a kind of Fabry-Perot interferometer, producing multiple interference of light rays propagating up and down within the cavity between the end face of the probe and the sample surface as it is outlined in Fig. 7.

If it is assumed that the interference comes from three different contributions, the resulting electric field E is given by the formula:

$$E = \sum_{n=1}^{3} E_n = \sum_{n=1}^{3} E_{0n}\, \mathrm{e}^{\mathrm{i}\alpha_n} \,, \tag{5}$$

where E_{0n} represents the corresponding amplitudes and α_n the phases, respectively. Here, E_1 is the electric field of the wave reflected at the end face of the fiber core, E_2 is the transmitted field after one reflection at the metallic surface of the sample, and E_3 is the transmitted field after two reflections from the sample surface and, in between, one reflection at the outer end face of the fiber probe.

This leads to the following expression for the intensity of the light finally detected by the photodiode:

$$\begin{aligned} I &= \left|E\right|^2 \\ &= E_{01}{}^2 + E_{02}{}^2 + E_{03}{}^2 + 2E_{01}E_{02}\cos(\alpha_1 - \alpha_2) + 2E_{02}E_{03}\cos(\alpha_2 - \alpha_3) + 2E_{01}E_{03}\cos(\alpha_1 - \alpha_3) \\ &= I_1 + I_2 + I_3 + 2\sqrt{I_1 I_2}\cos(\varphi_{12} + 4\pi(h_0 - z)/\lambda) + 2\sqrt{I_2 I_3}\cos(\varphi_{23} + 4\pi(h_0 - z)/\lambda) \\ &\quad + 2\sqrt{I_1 I_3}\cos(\varphi_{13} + 8\pi(h_0 - z)/\lambda). \end{aligned} \tag{6}$$

The intensity values $I_n = E_{0n}{}^2$ are the squares of the amplitudes of the different contributions and φ_{nm} are the relative phase differences of the interfering waves resulting from Fresnel reflection. The optical path difference corresponding to the last term in Eq. (6) is four times the distance between the two surfaces. This gives rise to the factor 8π. We assume that the phase change is zero for the internal reflection at the end face of the probe and it is π for the reflection at the metallic surface of the sample as well as for the outer reflection at the probe's end face. Under this consideration it follows that:

$$\varphi_{12} = \pi; \quad \varphi_{23} = 2\pi; \quad \varphi_{13} = 3\pi. \tag{7}$$

If we further assume that $I_1 \approx I_3$ Eq. (6) can be replaced by:

$$I \approx I_2 + 2I_1\left(1 - \cos(8\pi\,(h_0 - z)/\lambda)\right). \tag{8}$$

In Eq. (8) only the offset depends on the intensity I_2 which comes from the dominating single reflection at the sample surface. Consequently, a phase shift of 180° results if a distance change of $\lambda/8 \approx 100$ nm occurs. This agrees to the experimental result shown in Fig. 4 b). In comparison with a two beam reflection as considered in Eq. (4) the resolution according to Eq. (8) is two times better.

However, the fact that a significant part of the light reaches the fiber probe even after three reflections is due to the rather small numerical aperture of the probe.

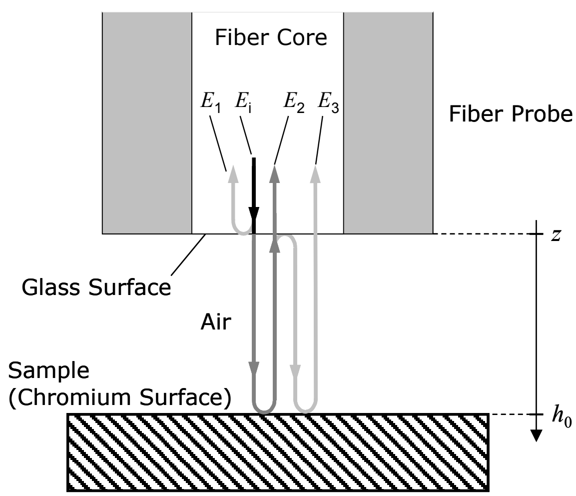

Fig. 7: Scheme of three beam interference resulting from multiple reflections.

For the signals shown in Fig. 4 approximately four interference fringes appear. This corresponds to a maximum deflection of 0.8 µm.

It shall be emphasized that the results shown in this study were just a first attempt in order to prove the principle of an oscillating probe. Although the configuration of the system was not optimized the results obtained are quite promising: a standard deviation of 3 nm could be reached without vibration isolation of the setup and the sensitivity of the sensor with respect to distance changes was demonstrated.

The measuring range corresponds to the maximum deflection of the bending beam and was limited in this study to a few micrometers. As a consequence the number of signal cycles from which the phase shift with respect to a synthetic reference signal has to be obtained is very limited. However an increase of the distance scanning range would lead to an increased number of cycles and finally results in an improved measuring accuracy.

In addition, due to the long shaft of the optical probe used for this study a height deflection of the bending beam is always accompanied by a lateral shift of the measuring spot. Since the length of the optical probe was approximately twice the length of the bending beam, the maximum lateral shift is about twice the maximum deflection of the bending beam, i.e. 1.6 µm in case of the results shown in Fig. 4. This is acceptable for a spot diameter of 10 micrometers but it should be reduced if a high lateral resolution is required. However, the lateral shift can be significantly reduced by modifying the geometry of the sensor configuration.
Another source of measuring uncertainty was, that due to the mechanical stimulation the optical probe tended to vibrate also in the transversal direction. It is to be expected that this effect can be also reduced by modifying the probe and sensor geometry.

5. CONCLUSIONS

In this contribution, a novel method of interferometric sensing has been introduced and verified by experimental investigations. Due to the mechanical depth scan, which is realized by use of a piezo-electrically driven bending beam the optical components of the system are less demanding.
Although the current realization may be optimized there are some promising advantages of the sensor principle. These can be summarized as follows:

- Since the end face of the single mode fiber acts as a confocal pinhole, the sensing principle is a combination of both confocal and interferometric sensing.
- In comparison with pure confocal sensors the so-called "interferometric gain"[8] should be mentioned, which allows a significantly better dynamic range:
  First, a confocal system is assumed, which determines the height value of an object point based on a depth scan. For an ideally aligned, flat surface area, which is located in the focal plane of an objective we suppose that the light intensity at the detector shows the maximum value $I = I_{max}$.
  If the object is moved, so that the surface area is far away from the focal plane of the confocal system the corresponding intensity is close to zero, i.e. $I \approx 0$. Consequently, the detector must be able to record the maximum intensity difference $\Delta I_{max} = I_{max}$. If a measuring object is scanned laterally and the reflectivity, the local surface slope or the local curvature changes, the maximum intensity and therefore the intensity difference ΔI obtained from the detector signal will be generally smaller. The minimum measurable ratio $S_c = \Delta I / \Delta I_{max}$ is called sensitivity in this context.
  For a two-beam interferometer the total intensity according Eq. (4) depends on both, the reference intensity I_1 and the object intensity I_2.
  If $I_1 = I_2 = I_0$ the maximum intensity difference, which has to be converted into voltage is $\Delta I_{max} = I_{max} = 4\, I_0$.
  Now, if the intensity I_2 in the measuring arm is changed by the same ratio as the intensity difference, which is to be obtained by the confocal sensor it follows that: $I_2 = S_c\, I_1 = S_c\, I_0$.
  Hence, for the intensity difference ΔI, which has to be tolerated by the interferometer and the sensitivity S_i the following relation results:
  $$\Delta I = 4\sqrt{I_1 I_2} = 4\sqrt{I_0^{\,2} S_c} = 4 I_0 \sqrt{S_c} \rightarrow \quad S_i = \Delta I / \Delta I_{max} = \sqrt{S_c} \quad . \tag{9}$$
  If, for example the intensity difference of a confocal signal is reduced by 10^{-4} of its maximum value, in the interferometric measurement this corresponds to a reduced modulation depth of the interference signal of 1% related to the maximum value. The consequence is that if a weak signal is to be measured by a confocal sensor a sensitivity of 10^{-4} is necessary while for an interferometric system only 10^{-2} is required.
- In our case a further improvement is possible since the offset term can be eliminated by appropriate high pass filtering. Furthermore, in contrast to detectors based on a CCD or CMOS line array, the digital resolution can be much higher, since only a single photo diode is used.
- Compared to low-coherence systems dispersion effects may be neglected because of the use of laser light sources.
- Therefore, the design of optical probes is quite straight forward, even if a high NA is required in order to reach a sub-micrometer lateral resolution or a high tolerance with respect to surface slope.
- The sensor principle can be realized on the basis of inexpensive standard components.

These advantages are accompanied by the necessity of an actuator for the mechanical oscillation. Whether these oscillations can be tolerated or not depends much on the mechanical arrangement of the measuring instrument which is used in combination with the optical sensor.

6. REFERENCES

1. O. Jusko, M. Neugebauer, H. Reimann, P. Drabarek, M. Fleischer, T. Gnausch, “Form measurements by optical and tactile scanning”, Proceedings of the SPIE, Vol. 7133, 71333A-71333A-12 (2008).
2. C. Dietz, M. Jurca „Eine Alternative zum Laser, Ein Weißlicht-Meßverfahren dringt in den Sub-µm-Bereich ein“, Sensor Magazin Nr. 4, 13-15 (1997).
3. A. Knüttel, F. Rammrath: “Spectral Coherence Interferometry (SCI) for fast and rugged industrial application“, CLEO/Europe, Conference Digest, Opt. Soc. Am., Paper TF2-1 (2007).
4. A. Ruprecht, C. Pruss, H. J. Tiziani, W. Osten, P. Lücke, A. Last, J. Mohr, P. Lehmann: Confocal microoptical distance-sensor: principle and design, SPIE Proceedings Vol. 5856, „Optical Measurement Systems for Industrial inspection“ 128-135 (2005).
5. P. Lücke, A. Last, J. Mohr, A. Ruprecht, C. Pruss, H. J. Tiziani, W. Osten, P. Lehmann: Confocal microoptical distance-sensor: realization and results, SPIE Proceedings Vol. 5856, „Optical Measurement Systems for Industrial inspection“ 136-142 (2005).
6. E. Papastathopoulos, K. Körner, W. Osten, “Chromatic confocal spectral interferometry with wavelet analysis”, SPIE Proceedings 6189 “Optical Sensing II”, (2006).
7. E. Papastathopoulos, K. Körner, W. Osten, “Chromatic confocal spectral interferometry”, Appl. Opt. **45** 8244-8252 (2006).
8. W. Lyda, K. Körner, W. Osten: “Einsatz der chromatisch-konfokalen spektralen Interferometrie zur Reduktion der Messunsicherheit bei chromatisch-konfokalen Topographiemessungen”, DGAO-Proceedings 2008 (ISSN: 1614 – 8436).
9. M. E. Brezinski: “Optical Coherence Tomography: Principles and Applications”, Academic Press 2006.
10. F. Depiereux, P. Lehmann, T. Pfeiffer, R. Schmitt: “Fiber-optical sensor with miniaturized probe head and nanometer accuracy based on spatially modulated low-coherence interferogram analysis”, Appl. Opt. **46** 3425-3431 (2007).
11. R. Schmitt, N. König, F. Depiereux: „Miniaturization and evaluation of fiber optic probes for low-coherence interferometry” Proceedings of the SPIE, Vol. 7003, 700304 (2008).